# Femtosecond laser inscription of asymmetric directional couplers for in-fiber optical taps and fiber cladding photonics

**Jason R. Grenier,* Luís A. Fernandes, and Peter R. Herman**

*Institute for Optical Sciences, and the Department of Electrical and Computer Engineering, University of Toronto, 10 Kings College Rd., Toronto, Ontario, M5S 3G4, Canada*

*j.grenier@utoronto.ca

**Abstract:** Precise alignment of femtosecond laser tracks in standard single mode optical fiber is shown to enable controllable optical tapping of the fiber core waveguide light with fiber cladding photonic circuits. Asymmetric directional couplers are presented with tunable coupling ratios up to 62% and bandwidths up to 300 nm at telecommunication wavelengths. Real-time fiber monitoring during laser writing permitted a means of controlling the coupler length to compensate for micron-scale alignment errors and to facilitate tailored design of coupling ratio, spectral bandwidth and polarization properties. Laser induced waveguide birefringence was harnessed for polarization dependent coupling that led to the formation of in-fiber polarization-selective taps with 32 dB extinction ratio. This technology enables the interconnection of light propagating in pre-existing waveguides with laser-formed devices, thereby opening a new practical direction for the three-dimensional integration of optical devices in the cladding of optical fibers and planar lightwave circuits.



**OCIS codes:** (060.2430) Fibers, single-mode; (130.5440) Polarization-selective devices; (130.7408) Wavelength filtering devices; (140.3390) Laser materials processing; (130.2755) Glass waveguides.

## References and links

1. L. Tong, R. R. Gattass, J. B. Ashcom, S. He, J. Lou, M. Shen, I. Maxwell, and E. Mazur, "Subwavelength-diameter silica wires for low-loss optical wave guiding," Nature **426**, 816–819 (2003).
2. R. Bergh, G. Kotler, and H. Shaw, "Single-mode fibre optic directional coupler," Electron. Lett. **16**, 260–261 (1980).
3. S. K. Sheem and T. G. Giallorenzi, "Single-mode fiber-optical power divider: encapsulated etching technique," Opt. Lett. **4**, 29–31 (1979).
4. T. Carmon, S. Y. T. Wang, E. P. Ostby, and K. J. Vahala, "Wavelength-independent coupler from fiber to an on-chip cavity, demonstrated over an 850nm span," Opt. Express **15**, 7677–7681 (2007).
5. A. M. Armani, R. P. Kulkarni, S. E. Fraser, R. C. Flagan, and K. J. Vahala, "Labelfree, single-molecule detection with optical microcavities," Science **317**, 783–787 (2007).
6. K. O. Hill, B. Malo, F. Bilodeau, D. C. Johnson, and J. Albert, "Bragg gratings fabricated in monomode photosensitive optical fiber by UV exposure through a phase mask," Appl. Phys. Lett. **62**, 1035–1037 (1993).
7. J.-L. Archambault, L. Reekie, and P. Russell, "100% reflectivity Bragg reflectors produced in optical fibres by single excimer laser pulses," Electron. Lett. **29**, 453–455 (1993).
8. T. Erdogan and J. E. Sipe, "Tilted fiber phase gratings," J. Opt. Soc. Am. A **13**, 296–313 (1996).

#238247 Received 20 Apr 2015; revised 15 Jun 2015; accepted 15 Jun 2015; published 17 Jun 2015

9. B. Malo, D. C. Johnson, F. Bilodeau, J. Albert, and K. O. Hill, "Single-excimer-pulse writing of fiber gratings by use of a zero-order nulled phase mask: grating spectral response and visualization of index perturbations," Opt. Lett. **18**, 1277–1279 (1993).
10. V. Bhatia and A. M. Vengsarkar, "Optical fiber long-period grating sensors," Opt. Lett. **21**, 692–694 (1996).
11. Y. Shevchenko, G. Camci-Unal, D. F. Cuttica, M. R. Dokmeci, J. Albert, and A. Khademhosseini, "Surface plasmon resonance fiber sensor for real-time and label-free monitoring of cellular behavior," Biosens. and Bioelectron. **56**, 359–367 (2014).
12. M. El-Amraoui, G. Gadret, J. C. Jules, J. Fatome, C. Fortier, F. Désévédavy, I. Skripatchev, Y. Messaddeq, J. Troles, L. Brilland, W. Gao, T. Suzuki, Y. Ohishi, and F. Smektala, "Microstructured chalcogenide optical fibers from As2S3 glass: towards new IR broadband sources," Opt. Express **18**, 26655–26665 (2010).
13. H. Lehmann, S. Brueckner, J. Kobelke, G. Schwotzer, K. Schuster, and R. Willsch, "Toward photonic crystal fiber based distributed chemosensors," Proc. SPIE **5855**, 419 (2005).
14. Y. Lai, K. Zhou, L. Zhang, and I. Bennion, "Microchannels in conventional single-mode fibers," Opt. Lett. **31**, 2559–2561 (2006).
15. C. Martelli, P. Olivero, J. Canning, N. Groothoff, B. Gibson, and S. Huntington, "Micromachining structured optical fibers using focused ion beam milling," Opt. Lett. **32**, 1575–1577 (2007).
16. R. Osellame, G. Cerullo, and R. Ramponi, *Femtosecond laser micromachining*, vol. 123 of *Topics in Applied Physics* (Springer-Verlag, 2012).
17. A. Dragomir, D. N. Nikogosyan, K. A. Zagorulko, P. G. Kryukov, and E. M. Dianov, "Inscription of fiber Bragg gratings by ultraviolet femtosecond radiation," Opt. Lett. **28**, 2171–2173 (2003).
18. S. J. Mihailov, C. W. Smelser, D. Grobnic, R. B. Walker, P. Lu, H. Ding, and J. Unruh, "Bragg gratings written in all-SiO2 and Ge-doped core fibers with 800-nm femtosecond radiation and a phase mask," J. Lightwave Technol. **22**, 94 (2004).
19. A. Martinez, M. Dubov, I. Khrushchev, and I. Bennion, "Direct writing of fibre Bragg gratings by femtosecond laser," Electron. Lett. **40**, 1170–1172 (2004).
20. G. D. Marshall, R. J. Williams, N. Jovanovic, M. J. Steel, and M. J. Withford, "Point-by-point written fiber-Bragg gratings and their application in complex grating designs," Opt. Express **18**, 19844–19859 (2010).
21. P. J. Lemaire, R. Atkins, V. Mizrahi, and W. Reed, "High pressure H2 loading as a technique for achieving ultrahigh UV photosensitivity and thermal sensitivity in GeO2 doped optical fibres," Electron. Lett. **29**, 1191–1193 (1993).
22. A. Martinez, Y. Lai, M. Dubov, I. Khrushchev, and I. Bennion, "Vector bending sensors based on fibre Bragg gratings inscribed by infrared femtosecond laser," Electron. Lett. **41**, 472–474 (2005).
23. J. Thomas, N. Jovanovic, R. G. Becker, G. D. Marshall, M. J. Withford, A. Tünnermann, S. Nolte, and M. J. Steel, "Cladding mode coupling in highly localized fiber Bragg gratings: modal properties and transmission spectra," Opt. Express **19**, 325–341 (2011).
24. L. A. Fernandes, J. R. Grenier, P. V. S. Marques, J. S. Aitchison, and P. R. Herman, "Strong birefringence tuning of optical waveguides with femtosecond laser irradiation of bulk fused silica and single mode fibers," J. Lightwave Technol. **31**, 3563–3569 (2013).
25. D. Grobnic, S. J. Mihailov, and C. W. Smelser, "Localized high birefringence induced in SMF-28 fiber by femtosecond IR laser exposure of the cladding," J. Lightwave Technol. **25**, 1996–2001 (2007).
26. R. G. Krämer, C. Voigtländer, E. Freier, A. Liem, J. U. Thomas, D. Richter, T. Schreiber, A. Tünnermann, and S. Nolte, "Femtosecond pulse inscription of a selective mode filter in large mode area fibers," Proc. SPIE **8601**, 86010S (2013).
27. N. Riesen, S. Gross, J. D. Love, and M. J. Withford, "Femtosecond direct-written integrated mode couplers," Opt. Express **22**, 29855–29861 (2014).
28. J. R. Grenier, L. A. Fernandes, P. V. Marques, J. S. Aitchison, and P. R. Herman, "Optical circuits in fiber cladding: femtosecond laser-written Bragg grating waveguides," Conference on Lasers and Electro-Optics - Laser Applications to Photonic Applications, (Optical Society of America, 2011), paper CMZ1.
29. J. R. Grenier, L. A. Fernandes, and P. R. Herman, "Femtosecond laser writing of optical edge filters in fused silica optical waveguides," Opt. Express **21**, 4493 (2013).
30. J. R. Grenier, M. Haque, L. A. Fernandes, K. Lee, and P. R. Herman, "Femtosecond laser inscription of photonic and optofluidic devices in fiber cladding, appearing in Springer Series in Optical Sciences 189" G. Marowsky ed. pp. 67–110 (2015).
31. A. M. Streltsov and N. F. Borrelli, "Fabrication and analysis of a directional coupler written in glass by nanojoule femtosecond laser pulses," Opt. Lett. **26**, 42–43 (2001).
32. K. Minoshima, A. Kowalevicz, E. Ippen, and J. Fujimoto, "Fabrication of coupled mode photonic devices in glass by nonlinear femtosecond laser materials processing," Opt. Express **10**, 645–652 (2002).
33. S. Eaton, W. Chen, L. Zhang, H. Zhang, R. Iyer, J. Aitchison, and P. R. Herman, "Telecom-band directional coupler written with femtosecond fiber laser," IEEE Photon. Technol. Lett. **18**, 2174–2176 (2006).
34. S. M. Eaton, M. L. Ng, R. Osellame, and P. R. Herman, "High refractive index contrast in fused silica waveguides by tightly focused, high-repetition rate femtosecond laser," J. Non-Crystalline Solids **357**, 2387–2391 (2011).
35. H. Zhang, S. Eaton, and P. R. Herman, "Single-step writing of Bragg grating waveguides in fused silica with an

#238247 Received 20 Apr 2015; revised 15 Jun 2015; accepted 15 Jun 2015; published 17 Jun 2015

externally modulated femtosecond fiber laser," Opt. Lett. **32**, 2559–2561 (2007).
36. Y. Shimotsuma, P. Kazansky, J. Oiu, and K. Hirao, "Self-organized nanogratings in glass irradiated by ultrashort light pulses," Phys. Rev. Lett. **91**, 247405 (2003).
37. R. Taylor, C. Hnatovsky, E. Simova, D. Rayner, V. Bhardwaj, and P. Corkum, "Femtosecond laser fabrication of nanostructures in silica glass," Opt. Lett. **28**, 1043–1045 (2003).
38. D. Dai, Z. Wang, and J. E. Bowers, "Ultrashort broadband polarization beam splitter based on an asymmetrical directional coupler," Opt. Lett. **36**, 2590–2592 (2011).
39. D. Marcuse, "Directional couplers made of nonidentical asymmetric slabs. Part II: Grating-assisted couplers," J. Lightwave Technol. **5**, 268–273 (1987).
40. L. A. Fernandes, J. R. Grenier, P. R. Herman, J. S. Aitchison, and P. V. S. Marques, "Stress induced birefringence tuning in femtosecond laser fabricated waveguides in fused silica." Opt. Express **20**, 24103–241114 (2012).
41. L. A. Fernandes, J. R. Grenier, P. R. Herman, J. S. Aitchison, and P. V. Marques, "Femtosecond laser fabrication of birefringent directional couplers as polarization beam splitters in fused silica," Opt. Express **19**, 11992–11999 (2011).

## 1. Introduction

With the preponderance of fiber optics in telecommunication, biomedical and sensing applications, there has been significant attention towards adding functionality directly within the fiber to avoid the packaging and assembly to discrete components. However, the fused silica cladding is a brittle, high temperature and transparent medium that has posed significant processing challenges in forming photonic cladding components that can evanescently access and integrate with the pre-existing core waveguide.

Various approaches have been explored to optically access the optical fiber core waveguide beyond the traditional means of end coupling at polished fiber facets. Thermal fusing of fiber enables the combination of pairs or multiple fibers to build a variety of fiber coupler types. More direct access to the core waveguide mode is found with flame thinning of the fiber cross-section, which has been scaled to sub-wavelength diameters [1]. Alternative means to thin the cladding are provided by lapping and polishing [2] or chemical etching [3] that have enabled broadband coupling, for example, to on-chip optical cavities [4] or provided a general means for evanescent sensing [5]. Laser processing directly within the fiber core waveguide has offered an attractive non-contact method of generating Bragg grating filters by phase-mask [6] or point-by-point direct writing [7] approaches, which have been used extensively in wavelength division multiplexing and optical fiber sensors. Alternatively, laser formation of tilted [8] or Type II Bragg gratings [9] as well as long period gratings [10] facilitate the coupling of the core waveguide light with the fiber cladding modes for broader benefits of spectral shaping and sensing, as well as enabling of plasmonic sensors on the cladding surface [11]. Further methods of building microholes or microfluidic channels to access the fiber core waveguide are highly varied, involving mechanical drilling [12], laser drilling [13], laser-chemical etching [14], and ion beam methods of milling [15].

In recent years there has been significant advances in applying femtosecond lasers to directly write buried optical waveguides and other optical devices in bulk glasses for their flexible integration into three-dimensional (3D) photonic circuits [16]. This fabrication approach has been extended to the core waveguide of optical fibers to form fiber Bragg gratings by means of phase-mask interference [17, 18] or direct writing [19, 20], offering strong responses in most types of glasses without the need for photosensitivity enhancement techniques [21]. The precise focal confinement of the laser interaction volume in direct writing has the further advantage of high resolution control in both positioning the refractive index structures to permit off-axis fiber Bragg gratings to enable direction sensitive bend sensing [22], as well as coupling to symmetry-specific cladding modes [23]. Alternatively, femtosecond laser-modification zones have been positioned adjacent to the core waveguide in the cladding region to tune the waveguide birefringence [24, 25], provide mode filtering in large mode area fibers [26], and create

#238247 Received 20 Apr 2015; revised 15 Jun 2015; accepted 15 Jun 2015; published 17 Jun 2015

mode selective couplers [27].

To facilitate the development of fiber cladding photonics, a high numerical aperture (NA) oil-immersion technique of femtosecond laser direct writing was developed to overcome the strong aberration and positional distortion when focusing outside the center-axis of the cylindrically shaped optical fiber [28, 29]. While Bragg grating waveguide (BGW) devices were demonstrated in the fiber cladding, the challenge of coupling light between the pre-existing single mode fiber (SMF) core waveguide and cladding photonic devices have not been fully developed. Preliminary approaches of forming optical fiber taps and directional couplers (DCs) in SMF28 fiber have been presented [30]. However, the opportunity for such monolithic and flexible 3D integration has been limited by the exceptionally tight alignment tolerances to meet with the pre-existing waveguide, as well as to account for the strong mismatch of propagation constants ($\Delta\beta \neq 0$) between the core and laser-formed waveguides that limit the available coupling.

This paper explores the design and fabrication of femtosecond laser-written asymmetric DCs in SMFs to form optical fiber taps that connect the core waveguide light with cladding waveguides without damage or modification to the core waveguide. The work builds on femtosecond laser writing of DCs in bulk glasses [31–33] to directly address the $\beta-$mismatch in waveguide propagation constants in the fiber. Real-time transmission monitoring during the coupler fabrication compensated for a typical $\pm 1$ μm positional alignment error in the waveguide offset position to the core waveguide and thereby provided a practical way to control and reproduce the desired coupler properties. Comprehensive evaluation of DC responses in the 1200 nm to 1700 nm wavelength spectrum are presented. The coupling coefficient and birefringence dependence as a function of the waveguide offset are examined and applied to tailor DC devices with variable coupling ratios that can serve as broadband couplers with minimal polarization dependence at shorter lengths to strongly isolating polarization selective taps of narrow bandwidth at longer lengths. In this way, femtosecond laser writing of DCs offers a precise method to create new types of in-fiber polarizers and spectral filters, as well as open opportunities to design and build fiber cladding photonics that connect with the fiber core waveguide.

## 2. Device fabrication and characterization

Single mode waveguide tracks were written into the cladding of Corning SMF-28 fiber as depicted in Fig. 1, following our previously reported fiber cladding writing technique [28]. The fiber was exposed to pulses of 130 nJ energy as provided by a frequency doubled femtosecond laser (IMRA America; μJewel D-400-VR) set to a 500 kHz pulse repetition rate, 522 nm wavelength, and 200 fs pulse duration. Linear polarization parallel to the scanning direction was selected to minimize birefringence and losses in the laser formed waveguides. An oil-immersion lens (AmScope PA100X) of $100\times$ (1.25 NA) magnification and working distance (0.13 mm) exceeding the fiber diameter offered aberration-free tight focusing with the advantage of distortion-free positioning of strongly confining waveguides to tolerances of $\pm 1$ μm relative to the core waveguide by monitoring laser back-reflection. A 10 cm length of stripped fiber was held taut in suspension and aligned parallel to an estimated $\pm 20$ μrad precision with the laser-scanning axis by monitoring the back-reflected laser beam. The fiber was scanned along the *-x* direction at 0.268 mm/s speed with respect to the laser beam focus position by a precise air-bearing motion control stage (Aerotech ABL1000). This direction was perpendicular to the grating compressor axis of the laser which was found to minimize waveguide losses according to pulse front tilt effects [29]. In this way (Fig. 1), waveguides of length, *L*, could be written at a center to center offset distance, *S*, away from the pre-existing SMF core waveguide to form an asymmetric DC. Directional couplers with offset distances of $S = 6$ μm to $S = 13.5$ μm were examined, ensuring that the laser waveguide was positioned close but outside

#238247 Received 20 Apr 2015; revised 15 Jun 2015; accepted 15 Jun 2015; published 17 Jun 2015

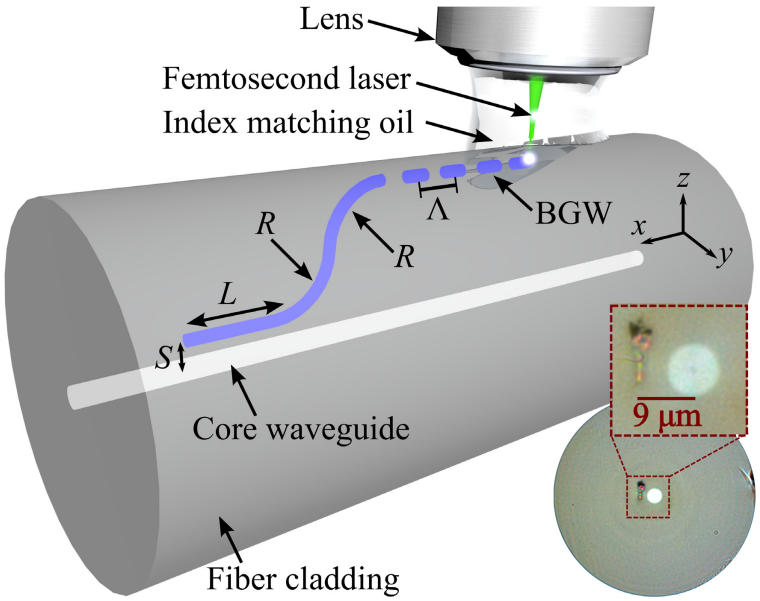


Fig. 1. Femtosecond laser writing of an asymmetric DC in an SMF with an oil-immersion lens. An optical micrograph (lower right corner) under backlighting shows the input cross-section of an SMF with a laser-formed waveguide (left) written with the laser incident from the top, and offset laterally by 9 μm from the core waveguide (right).

the core-waveguide (4.1 μm radius).

In select directional coupler devices, an additional output port was formed by writing a spur waveguide at an offset distance of 45 μm from the center of the fiber core, and following along an S-Bend path consisting of two circular arcs with 30 mm radius, $R$, to meet with the directional coupler. This writing order was essential to account for the contribution of S-Bend coupling and thereby provide reliable tuning of the coupler splitting ratio during real-time monitoring. The 30 mm radius was selected for a modest bend loss measured to be 1.7 dB/cm which was slightly higher than the simulated results presented by Eaton et al. [34] for similar exposure conditions. The straight spur waveguide was accessed by cleaving the fiber to define bar (core waveguide) and cross (laser-formed waveguide) ports to probe the DC characteristics. In other cases, the straight cross-port waveguide was formed into a 15 mm long, $\Lambda = 536$ nm pitch BGW, by modulating the laser exposure at 500 Hz and 60% duty cycle to create 500 Hz square-wave burst trains with an acousto-optic modulator [28,35]. In this way, the BGW would reflect the cross-port waveguide light on the Bragg resonance to a fiber circulator to probe the coupler efficiency as well as to provide a convenient means for determining the birefringence and polarization axis of the laser-formed waveguide.

Real-time monitoring was employed during the laser fabrication process by coupling unpolarized infrared light (Agilent: 83437A, 1200 nm to 1700 nm) into the SMF while continuously recording transmission of a single wavelength (typically 1550 nm) by an optical spectrum analyzer (OSA: Ando AQ6317B). In this way, the fabrication could be terminated at a desired coupler strength by manually blocking the laser beam, thereby overcoming the $\pm 1$ μm alignment uncertainties of the laser focus position. The slow writing speed of 0.268 mm/s was sufficient to fabricate couplers within 4% of a desired coupling ratio, corresponding to coupler lengths approximately within 150 μm of the ideal maximum or minimum transmission value. After fabrication, the transmission spectra of the DC bar and cross ports were recorded by probing

#238247 Received 20 Apr 2015; revised 15 Jun 2015; accepted 15 Jun 2015; published 17 Jun 2015

the device under test with unpolarized infrared light launched either through an end-coupled SMF or by free-space focusing with a 10× (0.16 NA) magnification lens. In the latter case, a broadband linear polarizer (Thorlabs: LPNIR) was used to preferentially excite parallel or perpendicular linearly polarized modes defined as having electric fields aligned parallel or perpendicular to the axis separating the two waveguides. This polarization alignment was precisely determined by the polarization splitting of the Bragg grating resonances [24, 28, 30] without generating any polarization variation over the short-length (<20 mm) straight fiber segments tested here. The beam profiles of the propagating modes were captured by coupling light from a tunable laser source (Photonetics: Tunics-BT, 1520 nm to 1600 nm) and imaging the fiber end-facet onto a phosphor-coated CCD camera (Spiricon: SP-1550M) with a lens of 60× (0.65 NA) magnification. All spectra were normalized relative to a direct fiber-to-fiber transmission and recorded with an optical spectrum analyzer (OSA: Ando AQ6317B). Index-matching oil was applied at all glass-fiber interfaces to reduce the Fresnel reflections and Fabry-Perot effects.

## 3. Results and discussion

A cross-sectional view of an optical fiber embedded with a DC is shown in the inset image in Fig. 1 for the example case where the writing laser, incident from the top surface, formed a waveguide at a lateral offset distance of $S = 9$ μm from the SMF core waveguide. Directional couplers were monitored in real time during laser writing by recording the normalized optical transmission through the SMF core waveguide. A comparison of 1550 nm wavelength transmission recorded for DCs with offset distances of $S = 15$ μm (blue line) and $S = 12$ μm (green line) are presented in Fig. 2, where the exposure time was converted to coupler length using the constant scanning speed. A stronger coupling with a deeper periodic oscillation in the transmission is noted with decreasing waveguide separation as expected, yielding a first half-cycle transmission drop of 1.5% (Point A) and 14% (Point B) for the $S = 15$ μm and $S = 12$ μm cases, respectively. The incomplete coupling arises from the mismatch in the waveguide propagation constants ($\Delta\beta$) between the SMF core and laser-formed waveguide. However, as the waveguide offset distance is decreased, the coupling coefficient increases and thereby permits greater coupling. The incomplete recovery of transmission to 100% in Fig. 2 is in part owing to radiation and cladding mode losses arising at the abrupt start and termination of the laser-written waveguide, and also to a discontinuity in the waveguide birefringence. These losses are observed to be distributed over the first oscillation cycle as the incoming fiber-core mode is reshaped by the directional coupler section to form into a steady-state supermode profile. An overall maximum coupling of 1.5% and 7.1% were inferred for the $S = 15$ μm and $S = 12$ μm separations, respectively, based on transmission probing of the cross-port (laser-formed) cladding waveguide. For the case of $S = 12$ μm separation, the fast DC oscillations ($\approx 2.2$ mm period) are accompanied with a longer 13.5 mm period oscillation that arises from birefringence induced by the laser writing, which is too weak to be observed in the $S = 15$ μm waveguide offset case. This birefringence arises from laser-generated nanogratings [36, 37] as well as a stress effect of the laser-formed waveguide on the SMF core waveguide [24]. Such long and short period oscillation beating is typical of asymmetric DCs with birefringence [38]. Femtosecond laser writing therefore offers the opportunity for flexible tailoring of such responses as in-fiber devices for the first time.

### *3.1. Asymmetric directional coupler design*

The design of in-fiber directional couplers can follow from traditional models of coupled mode theory for asymmetric and polarization dependent couplers, having power coupling ratios, $r_{V,H}$ at the cross-port (i.e. laser-formed cladding waveguide) according to the expression

#238247 Received 20 Apr 2015; revised 15 Jun 2015; accepted 15 Jun 2015; published 17 Jun 2015

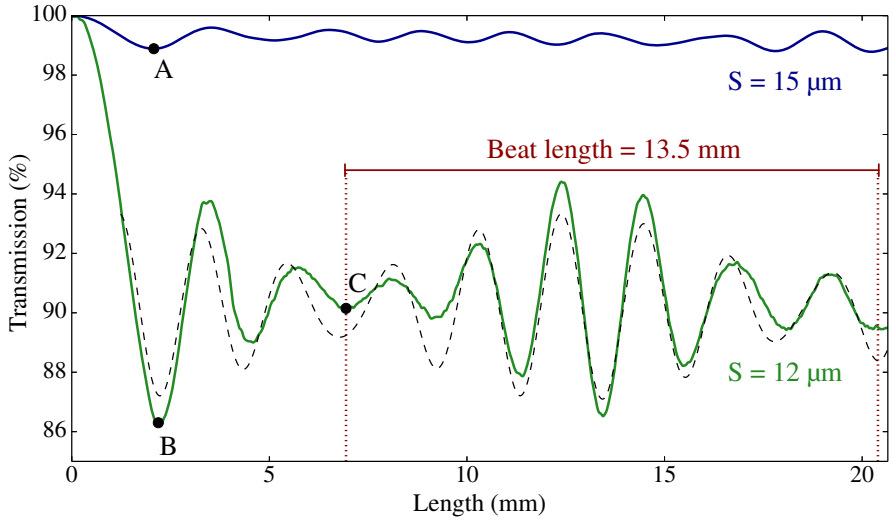


Fig. 2. Real-time recording plotted as DC length of the normalized optical transmissions of 1550 nm light through an SMF core waveguide during laser writing of a parallel waveguide offset by 15 μm (blue line) and 12 μm (green line), forming in-fiber asymmetric DCs. The dashed line shows the data fitted to Eq. (3).

$$r_{H,V}(\lambda) = \sigma^2_{H,V}(\lambda)\sin^2\left[\frac{\kappa_{H,V}(\lambda)}{\sigma_{H,V}(\lambda)}L\right], \tag{1}$$

The subscripts, $H$ and $V$, represent the horizontal and vertical linearly polarization eigenmodes, respectively, $\kappa$ is the coupling coefficient, $L$ is the coupling length, $\lambda$ is the wavelength, and $\sigma_{H,V}$ is the amplitude dephasing term, given by

$$\sigma_{H,V}(\lambda) = \sqrt{\frac{1}{1+\left(\frac{\Delta\beta_{H,V}(\lambda)}{2\kappa_{H,V}(\lambda)}\right)^2}}. \tag{2}$$

The non-zero $\beta-$mismatch is seen here to reduce the peak coupling and increase the effective coupling rate, $\kappa'_{H,V}(\lambda) = \frac{\kappa_{H,V}(\lambda)}{\sigma_{H,V}(\lambda)}$. Combining these factors with the insertion loss (IL), one finds Eq.( 3) to give a good representation (dashed line in Fig. 2) of the DC transmission as measured (solid line) through the SMF core waveguide versus the coupler length as shown in Fig. 2 for the case of an offset distance of 12 μm

$$\mathrm{T}(L) = \left(1 - IL - \left(\frac{r_V + r_H}{2}\right)\right)e^{-\alpha L}. \tag{3}$$

Here, values of $\kappa'_V = 1.40$ rad/mm and $\kappa'_H = 1.19$ rad/mm presented a best data fit (solid green) for the vertical and horizontal polarization eigenmodes, respectively, yielding a beat length of 14.96 mm that improved on the 13.5 mm beat length estimated in the figure. The zones of low modulation amplitude found at $L = 6.94$ mm (Point C) and $L = 20.4$ mm of Fig. 2 arise when the differential coupling phase $((2m-1)(\kappa'_V - \kappa'_H)L)$ accumulates an odd multiple of $\pi-$phase difference, for integer values of $m = 1$ and $m = 2$, respectively. At these points, the vertical and horizontal polarized light in the cross port oscillate out of phase, opening the

#238247 Received 20 Apr 2015; revised 15 Jun 2015; accepted 15 Jun 2015; published 17 Jun 2015

possibility for creating a polarization selective optical tap in the fiber cladding. The data fit with Eq. (3) further provided respective amplitude values of $\sigma_V^2 = 0.076$ and $\sigma_H^2 = 0.086$ for the vertical and horizontal polarizations together with an insertion loss of IL = 6.6% that underlie the minimum first half cycle transmission of 86% (Point B) as seen in Fig. 2. The fitted data also yielded a propagation loss of $\alpha = 7.2 \times 10^{-4}$ dB/cm for this coupler which is too small to be measurable or significant; however, this loss increased to $\alpha = 0.015$ dB/cm for a waveguide offset distance of $S = 6$ μm . Such low loss is expected as only a small portion of the total input light (one-half of 7.1% for the $S = 12$ μm offset) becomes coupled into the lossy ($\approx 0.6$ dB/cm) laser-formed waveguide.

The good representation of the DC data in Fig. 2 suggests that a wide latitude exists for designing asymmetric DCs for a broad range of in-fiber applications by managing the laser exposure to manipulate the coupling strength and birefringence effects in Eq. (2). To minimize losses from the laser-formed waveguides, shorter length DCs will be favored. Similarly, shorter length devices will minimize the polarization dependence of the DC, which in the case of $S =$ 12 μm offset can provide a range of coupling ratios up to 7.1% by terminating the laser writing length before the first half cycle length of 2.2 mm (Point B). Stronger coupling, faster oscillation frequency and reduced coupler length are shown below to be available as expected when the waveguide-offset position is further reduced. However, a practical limitation in device precision and reproducibility arises from the $\pm 1$ μm alignment uncertainty that can dramatically change the values of the coupling coefficient and amplitude dephasing factor. Real-time monitoring of the fiber transmission is therefore a highly effective and practical approach to terminate laser writing once the coupler length produces the desired coupling ratio.

The strong influence of the waveguide offset position on the directional coupling strength was readily assessed by real-time monitoring of unpolarized optical transmission of 1550 nm wavelength light through a SMF core waveguide as laser-formed waveguides were written at an angle of 0.24 mrad with respect to the core waveguide. This angle produced a chirped oscillation period along the device length to offer a local measure of the unpolarized effective coupling coefficient $\kappa' = ((\kappa'_V + \kappa'_H)/2)$ as a function of the lateral waveguide offset distance. This procedure was repeated several times and the data was filtered favoring those providing the highest peak $\kappa'$ values that was associated with the closest centering of the crossing waveguide with the central core waveguide. The results plotted in Fig. 3(a) vary the offset distances from $|S| = 6$ μm to $|S| = 13.5$ μm on the left (blue squares) and right (green squares) sides of the SMF core waveguide, showing high left-right symmetry. The one-sided error bars represent the variation over several similar sets of data. The experiment was repeated for vertical offset positions above (blue squares) and below (green squares) the SMF core waveguide and the results are presented in Fig. 3(b). A correction for the one-sided centering error ($\pm 1$ μm) was inferred for each angled waveguide scan by assessing the asymmetry of coupling data from waveguide arms positioned on opposite sides of the fiber core waveguide. The data shows the average effective coupling coefficient to increase exponentially with decreasing waveguide separation, consistent with coupling theory [39]. All data were well represented by exponential functions shown as dashed lines in Fig. 3. For the horizontal offset, the coupling data are left-right symmetric with respect to the anticipated center of the SMF core waveguide as expected by the left-right symmetry of the refractive index profile observed magnified in the inset in Fig. 1. This is not the case for the vertical offsets where Fig. 3(b) reveals an $\approx 25\%$ stronger coupling when the laser waveguide was positioned above (blue squares in Fig. 3(b)) compared to below (green squares in Fig. 3(b)) the SMF core waveguide. This asymmetry can be understood to arise from the asymmetric waveguide morphology shown in Fig. 1 (inset). A large vertical asymmetry arises from a strong negative refractive index zone formed above the guiding zone that is expected to inhibit the coupling when this zone is positioned between the laser-formed guiding zone

#238247 Received 20 Apr 2015; revised 15 Jun 2015; accepted 15 Jun 2015; published 17 Jun 2015

and the fiber core waveguide as seen for the green square data in Fig. 3(b). The laser-formed waveguide further shows a highly asymmetric index profile of 5:1 aspect ratio that can explain the 44% stronger coupling observed for vertical waveguide offset (Fig. 3(b)) in contrast to the horizontal offset (Fig. 3(a)) when the waveguides are formed near the cladding-core interface ($S \approx 6$ μm to 7 μm). Here, the positive index profile of the laser-formed waveguide is overlapping with the core waveguide only in the vertical offset case. However, this stronger coupling effect reverses for large vertical offset distances ($S > 8$ μm), compared with the equivalent horizontal offsets, owing to laser-induced stress zones of positive refractive index change being preferentially stronger and extending further (i.e. >20 μm) into the lateral direction [40].

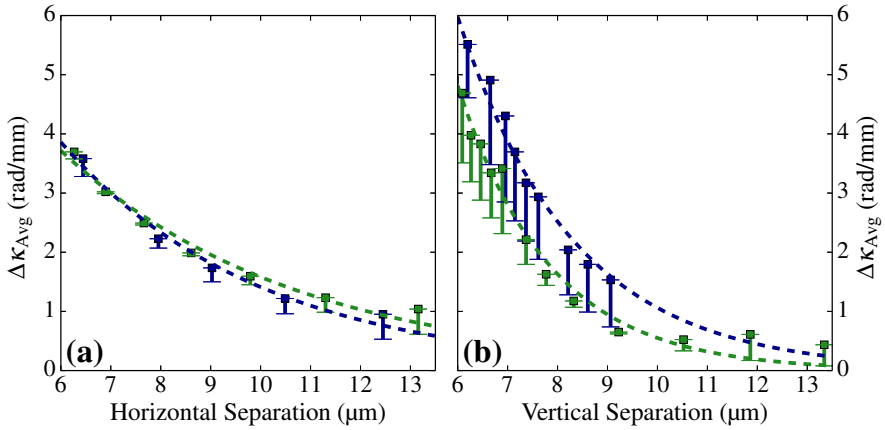


Fig. 3. Measured effective coupling coefficient ($\kappa'$) for unpolarized input light into asymmetric DCs consisting of a laser-formed waveguide placed **(a)** horizontally to the left (green squares) and right (blue squares) and **(b)** vertically above (blue squares) and below (green squares) the SMF core waveguide.

The asymmetric couplers presented here (Fig. 3) have $\approx 1.7\times$ larger effective coupling coefficients (e.g. $\approx 2.5$ rad/mm at $S = 8$ μm) than the values (e.g. $\approx 1.58$ rad/mm at $S = 8$ μm) reported previously for femtosecond laser-formed symmetric couplers in fused silica glass [41]. This increase arises from a reduction of the amplitude dephasing term in $\kappa' = \frac{\kappa_{H,V}}{\sigma_{H,V}(\lambda)}$ for the present case of non-zero $\beta-$mismatch according to Eq. (2). The polarization dependence of the effective coupling coefficients were also evaluated and found to remain nearly constant at $\kappa'_V - \kappa'_H = 0.24$ rad/mm and $\approx 0.38$ rad/mm for the respective horizontal and vertical waveguide offsets explored here.

### *3.2. Broadband optical fiber taps*

A consideration of the $\pm 1$ μm precision in the fiber alignment against the slopes in Fig. 3 suggests one would have a low sample-to-sample reproducibility in coupler response owing to a large random $\approx 20\%$ variation in controlling the $\kappa'$ value. Hence, real-time monitoring of the fiber transmission during laser writing was applied to demonstrate in-fiber DC devices serving as broadband optical taps and polarization-selective taps. The broadband optical tap relies on short coupler length to meet at a first minimum position for a range of weak or strong coupling conditions such as anticipated, for example, at the Point A and B positions in Fig. 2. Real-time monitoring was applied for a waveguide offset distance of $S = 9$ μm to stop the waveguide writing at such a maximum coupling position, found at $L = 0.680$ mm coupler length as presented in Fig. 4(a). A nearly uniform and broadband coupler is seen in the unpolarized

#238247 Received 20 Apr 2015; revised 15 Jun 2015; accepted 15 Jun 2015; published 17 Jun 2015

(black lines) transmission spectra for the bar (solid line) and cross (dashed line) ports. An $\approx 11\%$ coupling is provided to the cross port (laser-formed waveguide) over the 1400 nm to 1700 nm wavelength range, but which oscillates between 5% and 24% at wavelengths shorter than 1400 nm due to wider dispersion differences between the fiber core and laser-formed waveguides in this spectral region. The guided mode profile at 1526 nm wavelength (red circle) is shown in the inset image, confirming the appreciable alignment of the guided light over the SMF core waveguide (left) and only partially extending to the right towards the laser-formed waveguide position (marked by white +) as expected for this weaker coupling condition. The polarization dependence of the same coupler is presented in Fig. 4(b) where linearly polarized vertical (blue lines) and horizontal (green lines) spectra from the bar (solid lines) and cross (dashed lines) ports show only a small difference in their amplitudes over the 1400 nm to 1700 nm wavelength range. The minimal dispersion and polarization dependence displayed for this coupler is due to the short coupler length ($L = 0.680$ mm).

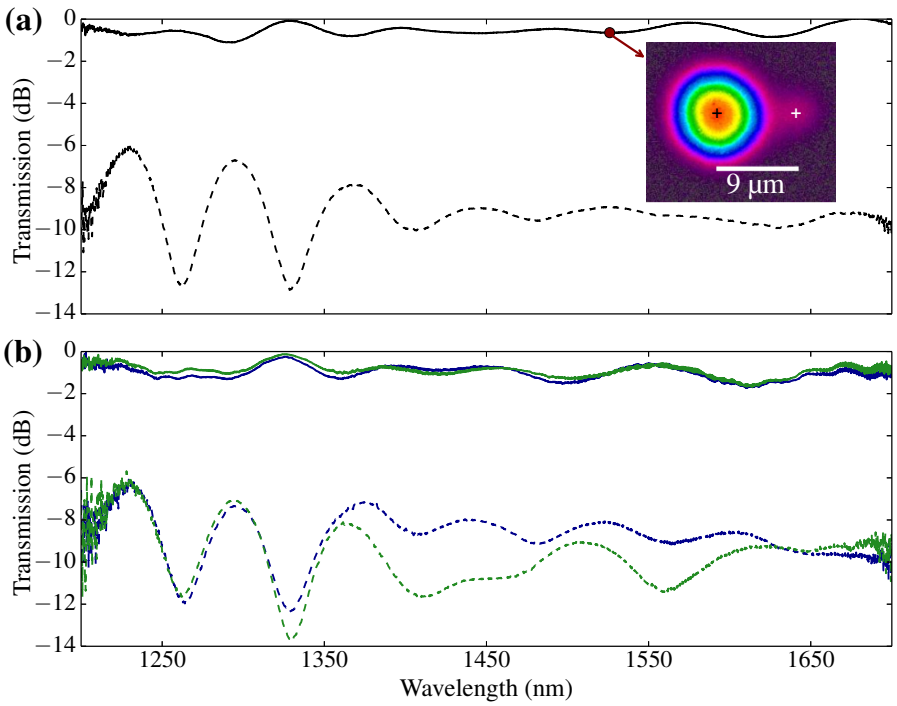


Fig. 4. Measured optical transmission spectra of **(a)** unpolarized (black) and **(b)** linearly polarized vertical (blue) and horizontal (green) light in the bar (solid lines) and cross (dashed lines) ports of an $L = 0.680$ mm length coupler with an $S = 9$ µm offset distance. Inset, an optical mode profile relative to the SMF core waveguide (black +) and laser-formed waveguide (white +) positions, for a cleaved DC with 1526 nm light launched into the SMF core waveguide.

### *3.3. Polarization selective taps*

The polarization selective tap requires a coupler length such that the accumulated coupling phase between the vertical and horizontal polarizations is equal to an odd integer multiple of $\pi$, for example, at the Point C in Fig. 2. Real-time monitoring was applied for waveguide offset distance of $S = 12$ µm to stop waveguide writing at $L = 16.88$ mm coupler length, near the

#238247 Received 20 Apr 2015; revised 15 Jun 2015; accepted 15 Jun 2015; published 17 Jun 2015

second ($m = 2$) polarization separation point. The optical transmission spectra for this device is shown in Fig. 5(a), where linearly polarized vertical (blue lines) and horizontal (green lines) light was recorded through the bar (solid lines) and cross (dashed lines) ports from 1250 nm to 1700 nm wavelengths. The long coupler length ($L = 16.88$ mm) here led to a rapid oscillation of the cross-port tapping on vertical and horizontal polarizations with period increasing with longer wavelength, from $\approx 40$ nm period at $\approx 1400$ nm to $\approx 80$ nm period at $\approx 1600$ nm. An imperfect phase alignment of the two polarization modes leads to a smaller polarization contrast ratio of less than 10 dB except at the resonance position of 1325.4 nm wavelength. Here, a strong contrast of 52% and 0.035% coupling of the vertical and horizontal polarization, respectively, provides a strong polarization selective tap with a peak extinction ratio of 32 dB and presenting greater than 29 dB isolation over a 1.2 nm bandwidth. Broader-band polarization selective taps require a shorter coupler length, which can be obtained by selecting the first ($m = 1$) polarization separation point or by decreasing the offset distance. Increasing the birefringence can further reduce the required coupler length, for example, by placing laser-formed stress tracks adjacent to the fiber core [24]. These methods can also be applied to tune the wavelength position of the polarization tap. The spectrum reveals that a peak coupling of 62% was obtained for horizontally polarized light at 1284 nm wavelength.

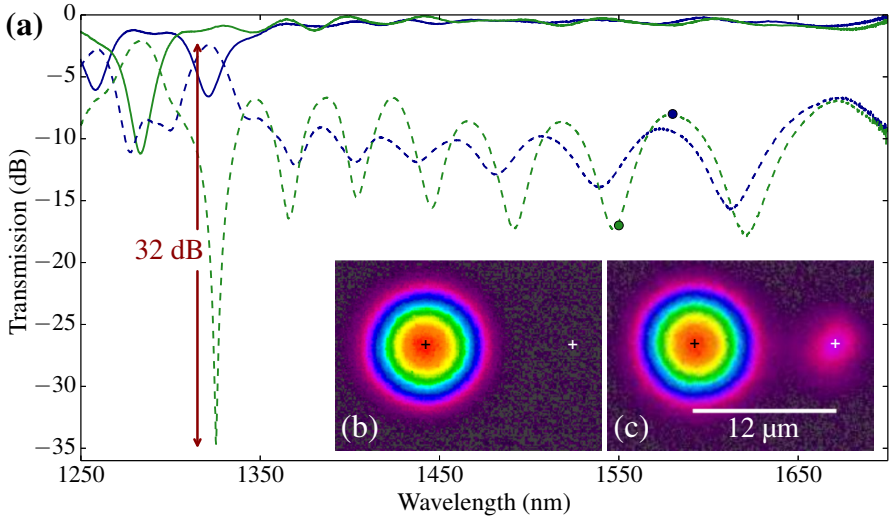


Fig. 5. **(a)** Measured optical transmission spectra of linearly polarized vertical (blue) and horizontal (green) light in the bar (solid lines) and cross (dashed lines) ports of an $L = 16.88$ mm length coupler with an $S = 12$ µm offset distance. Insets, an optical mode profile relative to the SMF core waveguide (black +) and laser-formed waveguide (white +) positions, for a cleaved DC with **(b)** 1550 nm and **(c)** 1580 nm light launched into the SMF core waveguide.

The mode profile of the polarization selective tap in Fig. 5(a) was imaged at local maximum and minimum coupling conditions found for vertically polarized light at 1550 nm and 1580 nm wavelengths, respectively, when launched into the SMF core waveguide and are shown in Fig. 5(b) and Fig. 5(c), respectively. In Fig. 5(b), guided light is not apparent around the laser-formed waveguide (marked by white +) owing to the small 2% (green circle in Fig. 5(a)) overall coupling as observed at 1550 nm wavelength whereas in Fig. 5(c) the modal light becomes visible at 1580 nm wavelength owing to the stronger observed 16% coupling (black

#238247 Received 20 Apr 2015; revised 15 Jun 2015; accepted 15 Jun 2015; published 17 Jun 2015

circle in Fig. 5(a)).

The present examples of femtosecond laser writing in fiber cladding demonstrate a novel extension of forming in-fiber DC devices to access new opportunities in fiber cladding photonics and sensing applications. The results extend beyond the DCs as laser-formed in bulk glasses [31–33] and enable the connection of laser-formed optical circuits with pre-existing waveguides as found extensively in conventional optical fiber and planar lightwave circuits. Despite the $\beta-$mismatch that limits the coupling (Eq. (2)) between the pre-existing SMF core and laser-formed waveguides, tunable coupling ratios up to 62% on one polarization (Fig. 5) were demonstrated. For large spectral coverage, a short coupler length of $L = 0.680$ mm was used to minimize dispersion effects and yield a coupler with wide 300 nm bandwidth (Fig. 4) in the telecommunication band. Conversely, longer coupler lengths yielded strongly modulated spectra which would find potential applications in wavelength division multiplexing and sensing. The laser-induced birefringence inherent in the laser writing process was further harnessed to produce strongly isolating (32 dB) polarization selective taps (Fig. 5(a)), which may be attractive for in-fiber polarimeter and polarization division multiplexing applications. Cascading multiple polarization selective taps could give way to in-fiber polarizers and polarization splitters or combining polarization selective taps with laser-formed in-fiber waveplates for polarization encoded quantum optic measurements. Coupled mode theory guided the coupler designs, while real-time monitoring of the fiber devices opened the necessary flexibility to compensate for the $\pm 1$ μm laser-position errors and generate desired spectral responses by controlling the coupler length.

## 4. Conclusion

Femtosecond laser pulses were strongly focused with an oil-immersion lens to offer distortion-free focusing inside the fiber cladding and form asymmetric directional couplers with the SMF core waveguide. Despite the $\beta-$mismatch, coupling ratios up to 62% were demonstrated in the 1200 nm to 1700 nm wavelength range. Short length couplers resulted in broadband coupling over a 300 nm range, while longer length couplers harnessed laser-induced waveguide and stress birefringence to form strongly isolating (32 dB) polarization selective taps. Real-time monitoring during laser fabrication was employed to overcome the acute coupling sensitivity to laser alignment errors of $\pm 1$ μm positional uncertainty and thereby open new practical directions for precise fabrication inside optical fibers and planar lightwave circuits. These advantages can now be exploited for coupling light to and from pre-existing waveguides paving the way towards an attractive alternate manufacturing method of flexibly adding optical functions or repairing and tuning in existing optical fiber and light circuits.

## Acknowledgments

Support from the National Science and Engineering Research Council of Canada is gratefully acknowledged.

#238247 Received 20 Apr 2015; revised 15 Jun 2015; accepted 15 Jun 2015; published 17 Jun 2015